SHORT COMMUNICATION

Intracellular Catabolism of an Antibody Drug Conjugate with a Non-Cleavable Linker

Brooke M Rock, Mark E Tometsko, Sonal K Patel, Kevin J Hamblett, William C Fanslow, Dan A Rock

Department of Pharmacokinetics and Drug Metabolism, Amgen, Inc, Seattle, WA
(BMR, DAR, SKP)

Therapeutic Innovation Unit, Amgen, Inc, Seattle, WA (KJH, MET, WCF)

DMD # 64253

Running Title Page

Running Title: In vitro catabolism of a non-cleavable ADC

Address for Correspondence:

Dan A Rock

1201 Amgen Court West

Seattle, WA 98119

Ph: (206) 265-7139

Fax: (206) 265-1149

E-mail: drock@amgen.com.

Text pages: 11

Tables: 0

Figures: 4

References: 16

Abstract words: 56

Introduction words: 787

Results/Discussion words: 796

Abbreviations:

Lys-MCC-DM1, Lysine-N⁻-4-(N-maleimidomethyl)cyclohexane-1-carboxylate)-N2-deacetyl-N2-(3-mercapto-1-oxopropyl)-maytansine; DM1,N2'-deacetyl-N2-(3-mercapto-1-oxopropyl)-maytansine; anti-CD70 Ab-MCC-DM1, antibody-N-succinimidyl4-(N-maleimidomethyl)cyclohexane-1-carboxylate- N2-deacetyl-N2-(3-mercapto-1-oxopropyl)-maytansine; DM4, N2'-deactyl-N2'-(4-mercapto-4-methylo-1-oxopentyl)-maytansine; ADC, antibody drug conjugate; SMCC, N-succinimidyl 4-(N-maleimidomethyl) cyclohexane-1-carboxylate; LC/MS/MS, liquid chromatography-tandem mass spectroscopy

2

Abstract

Antibody drug conjugates are emerging as a powerful class of anti-tumor agents with efficacy across a range of cancers; therefore, understanding the disposition of this class of therapeutic is crucial. Reported here, is a method to enrich a specific organelle (lysosome) to understand the catabolism of an anti-CD70 Ab-MCC-DM1, an antibody drug conjugate with a non-cleavable linker. With such techniques a higher degree of concentration-activity relationship can be established for in vitro cell lines which can aid in understanding the resultant catabolite concentrations necessary to exert activity.

Introduction

Antibody drug conjugates (ADCs) are agents that consist of a cytotoxic drug conjugated to a targeting antibody through various types of linkers (Alley et al., 2010; Erickson et al., 2010). A major design feature of an ADC is to maximize delivery of the cytotoxic agent to target tumor tissue, while minimizing delivery of the cytotoxin to untargeted tissues. The concept of treating cancer with an ADCs has gained momentum with the approval by the FDA of brentuximab vedotin (SGN-35, Adcetris®) for the treatment of Hodgkin's lymphoma and anaplastic large cell lymphoma and more recently, with the approval of trastuzumab emtanisine (T-DM1, Kadcyla®) for the treatment of human epidermal growth factor receptor-2 (HER2-) positive cancers (de Claro et al., 2012; Amiri-Kordestani et al., 2014).

Essentially there are two broad classes of ADC linkers; those that are chemically or enzymatically labile, referred to as cleavable and those that are chemically stable, referred to as non-cleavable. Cleavable (chemically labile) linkers are designed so that the ADC stays intact in circulation but releases the cytotoxin upon internalization by the target cell, usually due to a change in chemical environment in the cell or specific proteases in the cell which cleave the cytotoxin from the antibody (Fishkin et al., 2011; Han and Zhao, 2014). Subsequent tumor cell lysis results in ADC catabolites (cytotoxins) capable of permeating adjacent cells (bystander effect) which can be desirable in tumor environments with heterogeneous expression of the target antigen (Kovtun et al., 2006).

An ADC with a non-cleavable linker does not contain chemical functionalities that are readily susceptible to intracellular degradation, either in circulation or inside the target cell (Figure 1A). The general mechanism of action for an ADC with a non-cleavable linker requires the following (Figure 1B): 1) binding to the extracellular target/antigen, 2) endocytosis and trafficking to a lysosome, 3) degradation of the ADC, and 4) intracellular release of the active cytotoxin specie(s) where the mechanism of action of the cytotoxin (e.g. binding microtubulin)

4

leads to cell death. The effectiveness of the cytotoxin can be tuned by aligning physical-chemical properties of the linker but in general the cytotoxins have low permeability and rapid clearance limiting exposure to healthy tissues.

Antibody drug conjugates designed with non-cleavable linkers generally use a stable thioether, N-succinimidyl 4-(N-maleimidomethyl)cyclohexane-1-carboxylate (SMCC), with the maytansinoid moiety most commonly being, N2-deacetyl-N2-(3-mercapto-1-oxopropyl)-maytansine (DM1) (Erickson and Lambert, 2012). Conjugation of the cytotoxin occurs through the □-amino group lysine residues. Notably, this technology was utilized for Kadcyla®, where DM1 is linked to trastuzumab (a humanized monoclonal antibody) by a thioester bond between the sulfhydryl of DM1 and maleimide of SMCC (Lambert and Chari, 2014; Peddi and Hurvitz, 2014).

In theory for an ADC with the non-cleavable linker (SMCC), one main catabolite should be released after cellular processing, lysine-N−-MCC-DM1 (Lys-MCC-DM1). The formation of this single catabolite has been shown in vitro by dosing cells with [3][H]-ADC, and it was proposed that the formation of this catabolite occurs in the lysosome (Erickson et al., 2006; Erickson et al., 2012).

Presented here, is the development of a sensitive mass spectroscopy method to eliminate the need for radiolabeled ADC for investigation of in vitro catabolism. In addition, this work conclusively demonstrates catabolism of anti-CD70 Ab-MCC-DM1 (Figure 1A) to the active catabolite Lysine-MCC-DM1 occurs in the lysosomal compartment.

DMD # 64253

Materials and Methods

Materials

Bafilomycin A1 was purchased from ACROS Organics (West Chester, PA). Lys-MCC-DM1 was obtained from ImmunoGen (Waltham, MA). Anti-CD70 Ab-MCC-DM1 and anti-ST Ab-MCC-DM1 (control antibody) wereobtained from Amgen, Inc (Thousand Oaks, CA), and the concentration of anti-CD70 Ab-MCC-DM1 was stoichiometrically calculated to the moles of DM1 attached to the antibody [DM1 equivalents]. All commercial solvents Sigma-Aldrich (St. Louis, MO) were of LC/MS analytical grade. Lysosome Enrichment Kit for tissue and cultured cells, was purchased from Thermo Scientific (Waltham, MA). 786-0 cells were originally obtained from ATCC (Manassas, VA) and passaged in RPMI + 10% FBS. All other materials were purchased from Sigma-Aldrich (St. Louis, MO), unless specified.

Cellular activity of ADC treated 786-0 cells

786-0 cells were cultured in a 96-well tissue culture plate and incubated at 37°C, 5% CO_2 for approximately 4-6 hours. Serial dilutions of anti-CD70 Ab-MCC-DM1 were added to wells, as well as a control conjugate (no antigen binding). Following a 96 hr exposure cellular ATP level, which correlates to cell number, was assessed using the CellTiter Glo reagent (Promega, Madison, WI). Luminescence was measured using an Envision plate reader (Perkin Elmer, Waltham, MA).

Lysosome Enrichment from ADC treated 786-0 cells

ADC treated 786-0 cells from a 6-well plate were trypsinized and combined with trypsinized untreated 786-0 cells from a T175 flask. The cells were centrifuged, the supernatant aspirated and pellet washed with cold PBS. The cells were centrifuged once more, the supernatant aspirated and pellet resuspended in homogenization buffer (with added protease inhibitors). The cell suspension was then transferred to a Dounce tissue grinder and

6

homogenized on ice by performing 180 strokes to achieve about 80-90% cell breakage. The lysate was centrifuged to remove unbroken cells and nuclei. The resulting post nuclear supernatant was diluted in OptiPrep gradient media to a final concentration of 15% OptiPrep media. A discontinuous density gradient was prepared in descending concentrations (30%, 27%, 23%, 20%, 17%). The sample containing 15% Optiprep media was layered on top of the gradient and sample ultracentrifuged at 55,000 rpm for 2 hrs. The lysosome band was removed and frozen for further analysis by mass spectrometry.

Sample preparation and analytical method for measurement of ADC catabolite

Each sample (total cell lysate or enriched lysosome fraction) was prepared by adding 1 mL of lysis buffer (50 mM Tris HCl, 100 mM NaCl, 0.1% Triton X-100, pH 7.4), and the sample was transferred to a 15 mL glass conical test tube. Then 1 mL of ethyl acetate, (containing 1nM internal standard, DM4) was added to extract catabolites, a total of three times, and each aliquot was transferred to a new glass conical test tube. Ethyl acetate extractions were complete dried under nitrogen. Samples were reconstituted in 50/50 mixture of water/acetonitrile (50 uL) before analysis by LC/MS/MS. The LC/MS/MS analysis was performed using a Thermo Scientific Quantum (TSQ) triple quadrupole mass analyzer in line with a Thermo Accela Ultra Performance Liquid Chromatography (UPLC) separation system (Thermo Scientific, Waltham, MA). Analytes were separated on a Kinetex 2.6u C18 50x2.1mm column. The peaks eluted using a linear gradient at 0.2 mL/min and mobile phases A: 0.1% formic acid in water and B: 0.1% formic acid in acetonitrile. The gradient started at 80% A (0-0.5 min). Solvent B was linearly increased from 20% at 0.5 min to 100% at 4 min. The total run time was 6 min. The precursor > fragment ions monitored were Lys-MCC-DM1 (1103 > 485 m/z) and DM4 (795 > 547 m/z). TSQ mass analyzer was operated at unit mass resolution (FWHM set to 0.7 for both Q1 and Q3). The ion transfer capillary temperature was set at 325 °C. The other ESI source parameters for each instrument were optimized for flow rate of 0.2 mL/min. The LLOQ for the

DMD # 64253

method was 0.5 pg/mL. Data acquisition and analysis were accomplished with Xcalibur software

versions 1.4 (Thermo Electron Corporation, Waltham, MA).

Results

In vitro potency of anti-CD70 Ab-MCC-DM1 in 786-0 cells and formation of Lys-MCC-DM1 in total cell lysate

Anti-CD70 Ab-MCC-DM1 (0-30 nM [DM1 equivalents]) was assayed for its cytotoxic potency against CD70-positive 786-0 cells. The ADC inhibited cell growth with an approximate IC_{50} value of 1 nM [DM1 equivalents] upon a 96 hr exposure (Figure 2A). In contrast to anti-CD70 Ab-MCC-DM1, the control conjugate exhibited no cell growth inhibition. In a similar experimental setup, the total cellular Lys-MCC-DM1 was measured over a time course (Figure 2B) following exposure to varying concentrations of anti-CD70 Ab-MCC-DM1. The results indicated that the formation of Lys-MCC-DM1 was both concentration and time-dependent. Measurable amounts of Lys-MCC-DM1 were not detected until 12 hours after addition of anti-CD70 Ab-MCC-DM1. Control conjugate did not generate any measurable amounts of Lys-MCC-DM1 over 48 hours.

Effect of a lysosomal inhibitor on cellular toxicity induced by anti-CD70 Ab-MCC-DM1

To examine whether uptake and processing of anti-CD70 Ab-MCC-DM1 through the lysosomes was necessary for the activity against 786-0 cells, cellular toxicity was measured in the presence of varying concentrations of bafilomyocin A1. Bafillomyocin A1 selectively inihibits V-ATPase, a proton pump present in the endosomes and lysosomes, which leads to neutralization of the pH in these vesicles (Bowman et al., 1988). A dose-response for cellular activity was observed over a concentration range of 0-100 nM bafilomyocin A1 (Supplemental Figure 1). The concentration of Lys-MCC-DM1 formed was also measured in the same experiment and the results correlated to the dose response observed in the cellular activity assay (Figure 3). These findings provide mechanistic support for the importance of lysosomal processing in the activation of anti-CD70 Ab-MCC-DM1.

Enrichment of lysosome fractions from anti-CD70 Ab-MCC-DM1 treated 786-0 cells

To further investigate the role of lysosomal processing in the catabolism of anti-CD70 Ab-MCC-DM1, enrichment of and isolation of the lysosomal fraction was performed. After enrichment for the lysosomal fraction, the concentration of Lys-MCC-DM1 was measured by LC/MS/MS. The concentration of Lys-MCC-DM1 correlated well with the markers of lysosomal activity (Cathepsin D, Lamp1 and Rab9, Figure 4) in fractions 1-5. The total amount of Lys-MCC-DM1 found in the lysosomal fractions was 0.12 ng/200,000 cells, in comparison to the total cell lysate where the amount was 0.69 ng/200,000 cells. Therefore, 17% of the total amount of Lys-MCC-DM1 resides in the lysosome 24 hr after treatment with the anti-CD70 Ab-MCC-DM1. The remaining Lys-MCC-DM1 was accounted for in the cellular supernatant and extraction from the cell pellet after lysosomal enrichment, with a total recoveries ranging from 89-94% (Supplemental Table 1).

Discussion

Antibody drug conjugates are emerging as a powerful class of anti-tumor agents (Wakankar et al., 2011; Lin et al., 2013). Understanding the site of catabolism, and possible rate limiting steps in the cellular distribution of the cytotoxic catabolite is crucial, especially for ADCs with non-cleavable linkers that are dependent on cellular catabolism processes to generate the cytotoxin (Doronina et al., 2006; Erickson et al., 2006; Erickson et al., 2010). Reported here is the catabolism of anti-CD70 Ab-MCC-DM1, an ADC with a non-cleavable linker (SMCC). To investigate the catabolism, 786 0 cells were treated with an antigen-specific anti-CD70 Ab MCC-DM1. High resolution mass spectroscopy scanning methods coupled with multiple mass defect filtering were utilized to search for catabolites, only one catabolite was detected, Lysine-MCC-DM1 (data not shown). Moreover, the total Lys-MCC-DM1 concentrations correlated with cell growth inhibition.

Treatment of cells with a known lysosomal protease inhibitor bafilomyocin indicated the importance of the lysosomal compartment in the breakdown of anti-CD70 Ab-MCC-DM1, similar to a previous report using a different antibody-MCC-DM1 molecule. To further the understanding of the formation of Lys-MCC-DM1, enrichment of the lysosomes from the cellular components was performed. Although this is a well-established technique (Gjoen, 1997), this is the first report of enrichment of the lysosomal fraction after catabolism of an ADC for identification of catabolites. No Lys-MCC-DM1 was detectable outside the cell in the supernatant consistent with the low permeability of Lys-MCC-DM1 which was measured in LLC-PK1 cells (Supplemental Table 2). This finding showcases a distinction of this class of non-cleavable ADC having little potential for bystander effect due to sequestration of the Lys-MCC-DM1 in the cell.

Previously, it has been reported that Lys-MCC-DM1 is a circulating species in serum, in both preclinical ADME studies as well as in the clinic for T-DM1, an ADC with the same linker-drug combination studied here (Shen et al., 2012). With numerous other ADCs in clinical trials with non-cleavable linkers (Sassoon and Blanc, 2013), understanding the mechanism in which Lys-MCC-DM1 is formed is essential. Given that ADCs are complex molecule composed of both large molecule and small molecule entities, the findings here add to the overall understanding of cellular disposition of an ADC with a non-cleavable linker. Furthermore, experimental design with this method can be used to derive a link between ADC catabolism and resultant catabolite concentrations necessary to exert activity.

Authorship Contributions

Participated in research design: B.Rock, D.Rock, Patel, Hamblett, Tometsko, Fanslow

Conducted experiments: B.Rock, Patel, Tometsko

Contributed new reagents or analytic tools: none

Performed data analysis: B.Rock, Tometsko, Hamblett

Wrote or contributed to the writing of the manuscript: B.Rock, D.Rock

DMD # 64253

References

Alley SC, Okeley NM, and Senter PD (2010) Antibody-drug conjugates: targeted drug delivery for cancer. *Curr Opin Chem Biol* **14:**529-537. doi: 510.1016/j.cbpa.2010.1006.1170. Epub 2010 Jul 1017.

Amiri-Kordestani L, Blumenthal GM, Xu QC, Zhang L, Tang SW, Ha L, Weinberg WC, Chi B, Candau-Chacon R, Hughes P, Russell AM, Miksinski SP, Chen XH, McGuinn WD, Palmby T, Schrieber SJ, Liu Q, Wang J, Song P, Mehrotra N, Skarupa L, Clouse K, Al-Hakim A, Sridhara R, Ibrahim A, Justice R, Pazdur R, and Cortazar P (2014) FDA approval: ado-trastuzumab emtansine for the treatment of patients with HER2-positive metastatic breast cancer. *Clin Cancer Res* **20:**4436-4441. doi: 4410.1158/1078-0432.CCR-4414-0012. Epub 2014 May 4430.

Bowman EJ, Siebers A, and Altendorf K (1988) Bafilomycins: a class of inhibitors of membrane ATPases from microorganisms, animal cells, and plant cells. *Proc Natl Acad Sci U S A* **85:**7972-7976.

de Claro RA, McGinn K, Kwitkowski V, Bullock J, Khandelwal A, Habtemariam B, Ouyang Y, Saber H, Lee K, Koti K, Rothmann M, Shapiro M, Borrego F, Clouse K, Chen XH, Brown J, Akinsanya L, Kane R, Kaminskas E, Farrell A, and Pazdur R (2012) U.S. Food and Drug Administration approval summary: brentuximab vedotin for the treatment of relapsed Hodgkin lymphoma or relapsed systemic anaplastic large-cell lymphoma. *Clin Cancer Res* **18:**5845-5849. doi: 5810.1158/1078-0432.CCR-5812-1803. Epub 2012 Sep 5847.

Doronina SO, Mendelsohn BA, Bovee TD, Cerveny CG, Alley SC, Meyer DL, Oflazoglu E, Toki BE, Sanderson RJ, Zabinski RF, Wahl AF, and Senter PD (2006) Enhanced activity of monomethylauristatin F through monoclonal antibody delivery: effects of linker technology on efficacy and toxicity. *Bioconjug Chem* **17:**114-124.

Erickson HK and Lambert JM (2012) ADME of antibody-maytansinoid conjugates. *AAPS J* **14:**799-805. doi: 710.1208/s12248-12012-19386-x. Epub 12012 Aug 12249.

Erickson HK, Lewis Phillips GD, Leipold DD, Provenzano CA, Mai E, Johnson HA, Gunter B, Audette CA, Gupta M, Pinkas J, and Tibbitts J (2012) The effect of different linkers on target cell catabolism and pharmacokinetics/pharmacodynamics of trastuzumab maytansinoid conjugates. *Mol Cancer Ther* **11:**1133-1142. doi: 1110.1158/1535-7163.MCT-1111-0727. Epub 2012 Mar 1139.

Erickson HK, Park PU, Widdison WC, Kovtun YV, Garrett LM, Hoffman K, Lutz RJ, Goldmacher VS, and Blattler WA (2006) Antibody-maytansinoid conjugates are activated in targeted cancer cells by lysosomal degradation and linker-dependent intracellular processing. *Cancer Res* **66:**4426-4433.

Erickson HK, Widdison WC, Mayo MF, Whiteman K, Audette C, Wilhelm SD, and Singh R (2010) Tumor delivery and in vivo processing of disulfide-linked and thioether-linked antibody-maytansinoid conjugates. *Bioconjug Chem* **21:**84-92. doi: 10.1021/bc900315y.

Fishkin N, Maloney EK, Chari RV, and Singh R (2011) A novel pathway for maytansinoid release from thioether linked antibody-drug conjugates (ADCs) under oxidative conditions. *Chem Commun (Camb)* **47:**10752-10754. doi: 10710.11039/c10751cc14164c. Epub 12011 Aug 10726.

Gjoen T, et. al. (1997) Lysosomes and endocytosis. , in: *Subcellular fractionation: A practical approach* (Graham JMaR, D ed), pp 169-200, IRL Press Limited, Oxford, England.

Han TH and Zhao B (2014) Absorption, distribution, metabolism, and excretion considerations for the development of antibody-drug conjugates. *Drug Metab Dispos* **42:**1914-1920. doi: 1910.1124/dmd.1114.058586. Epub 052014 Jul 058521.

DMD # 64253

Kovtun YV, Audette CA, Ye Y, Xie H, Ruberti MF, Phinney SJ, Leece BA, Chittenden T, Blattler WA, and Goldmacher VS (2006) Antibody-drug conjugates designed to eradicate tumors with homogeneous and heterogeneous expression of the target antigen. *Cancer Res* **66:**3214-3221.

Lambert JM and Chari RV (2014) Ado-trastuzumab Emtansine (T-DM1): an antibody-drug conjugate (ADC) for HER2-positive breast cancer. *J Med Chem* **57:**6949-6964. doi: 6910.1021/jm500766w. Epub 502014 Jul 500710.

Lin K, Tibbitts J, and Shen BQ (2013) Pharmacokinetics and ADME characterizations of antibody-drug conjugates. *Methods Mol Biol* **1045:117-31.:**10.1007/1978-1001-62703-62541-62705_62707.

Peddi PF and Hurvitz SA (2014) Ado-trastuzumab emtansine (T-DM1) in human epidermal growth factor receptor 2 (HER2)-positive metastatic breast cancer: latest evidence and clinical potential. *Ther Adv Med Oncol* **6:**202-209. doi: 210.1177/1758834014539183.

Sassoon I and Blanc V (2013) Antibody-drug conjugate (ADC) clinical pipeline: a review. *Methods Mol Biol* **1045:1-27.:**10.1007/1978-1001-62703-62541-62705_62701.

Shen BQ, Bumbaca D, Saad O, Yue Q, Pastuskovas CV, Khojasteh SC, Tibbitts J, Kaur S, Wang B, Chu YW, LoRusso PM, and Girish S (2012) Catabolic fate and pharmacokinetic characterization of trastuzumab emtansine (T-DM1): an emphasis on preclinical and clinical catabolism. *Curr Drug Metab* **13:**901-910.

Wakankar A, Chen Y, Gokarn Y, and Jacobson FS (2011) Analytical methods for physicochemical characterization of antibody drug conjugates. *MAbs* **3:**161-172. Epub 2011 Mar 2011.

15

DMD # 64253

Figure Legends

Figure 1. (A) General structure of non-cleavable antibody maytansiod conjugate **(B)** Mechanism of ADC activity where, (A) localization of ADC to the tumor cell, (B) binding of ADC to specific antigen, (C) internalization into the endosome release the antigen from ADC, (D) catabolism of ADC in the lysosome, (E) release of Lys-MCC-DM1 into the cytoplasm, and (F) binding of Lys-MCC-DM1to tubulin resulting in cell cycle arrest and apoptosis.

Figure 2. (A) Serial dilutions of anti-CD70 Ab-MCC-DM1 were added 786-0 cells, as well as a control ADC (no antigen binding). Following a 96 hr exposure cell growth inhibition was assessed using the CellTiter Glo reagent. The total luminescence, which correlates to cell number, is plotted against concentration of anti-CD70 Ab-MCC-DM1, [DM1 equivalents] **(B)** Accumulation of Lys-MCC-DM1 in 786-0 cells treated with varying concentrations of anti-CD70 Ab-MCC-DM1 (0-30 nM [DM1 equivalents]) over 48 hr. The total amount (ng) of Lys-MCC-DM1 per approximately 200,000 cells is plotted against time.
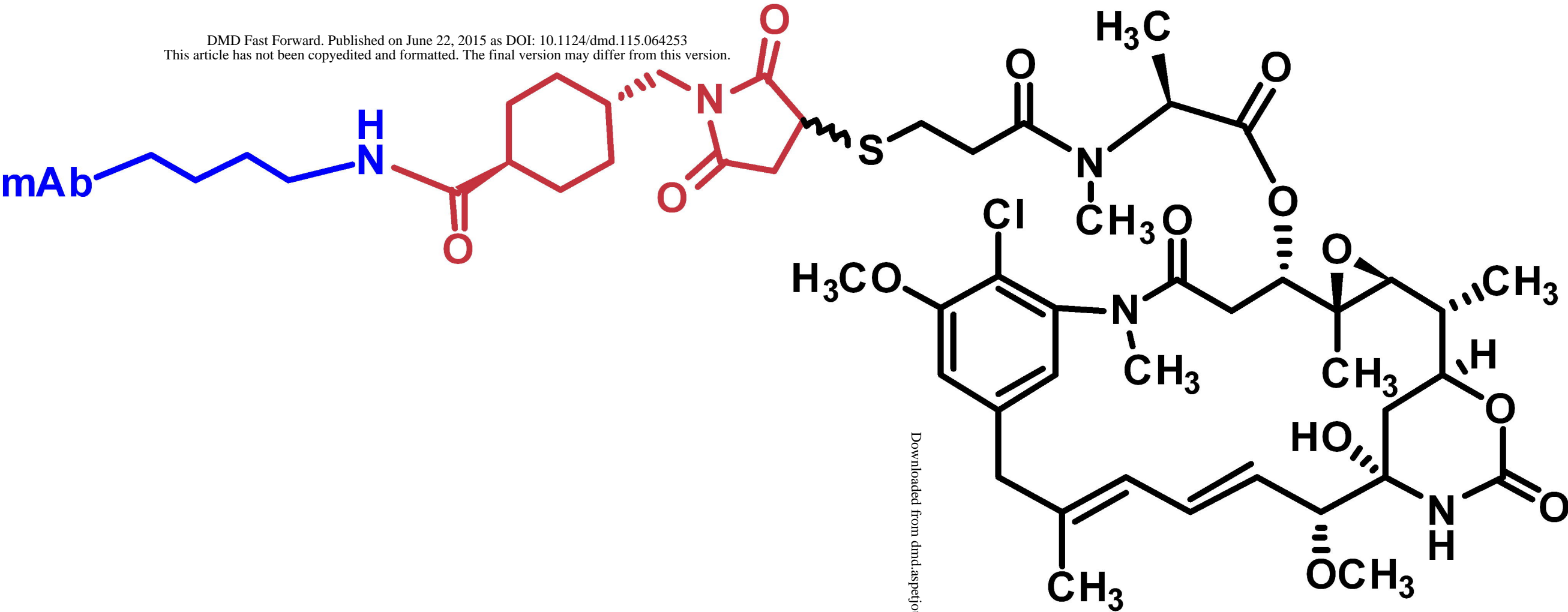
Figure 3. Formation of Lys-MCC-DM1 in the presence of Baflomyocin (0-100 nM) and 10 nM [DM1 equivalents] of anti-CD70 Ab-MCC-DM1 for 24 hr.

Figure 4 (A) Analysis of subcellular fractions from 786-0 cells, western blots showing lysosome/endosome enrichment (cathepsin D, Lamp1 and Rab 9) in top fractions with minimum contamination from mitochondria (COX IV). **(B)** Amount of Lys-MCC-DM1 measured in enriched lysosomes fractions after 10 nM [DM1 equivalents] of anti-CD70 Ab-MCC-DM1 treatment for 24 hr
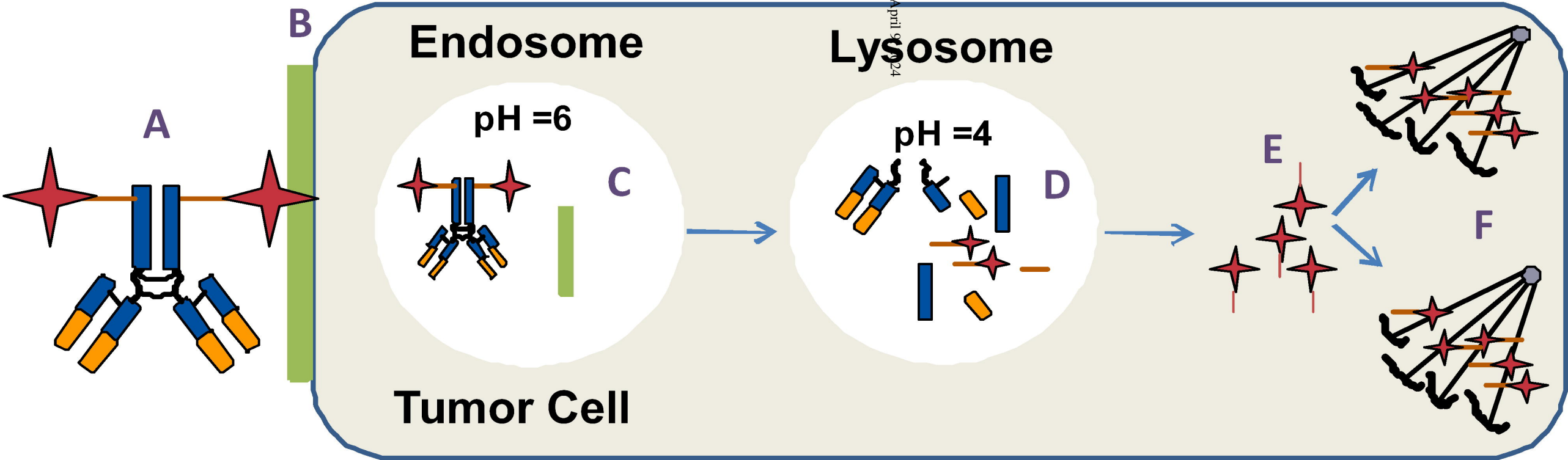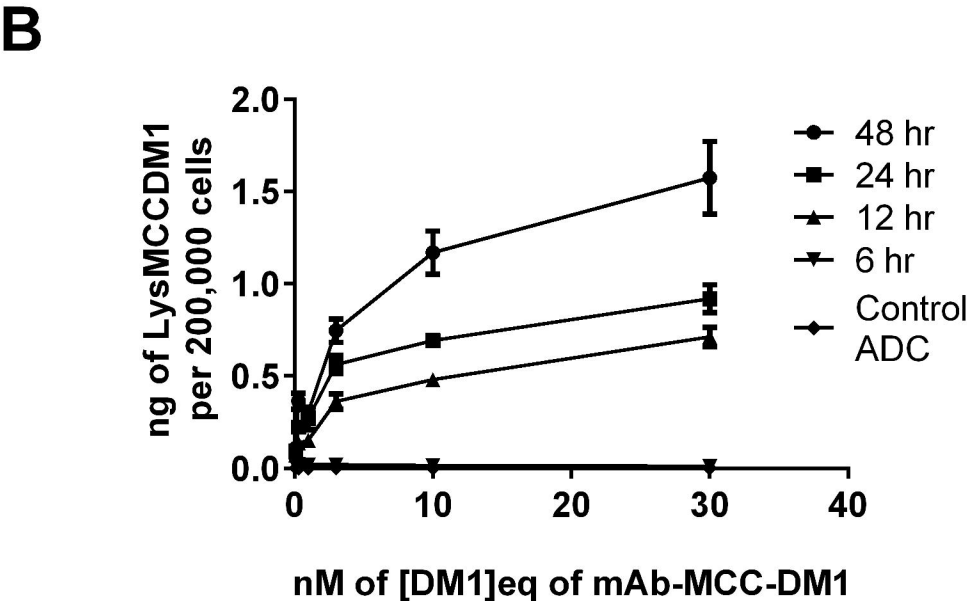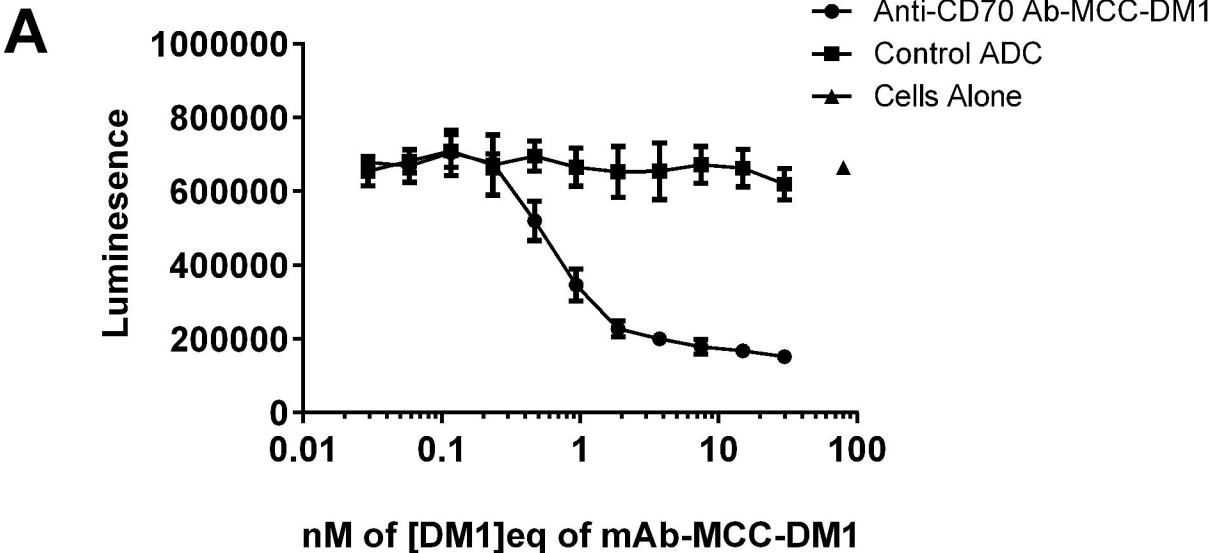
16

Figure 1

Figure 2

Figure 3

Figure 4

A

Cathepsin D

Lamp 1

Rab 9

COX IV

1 2 3 4 5 6 7 8 9 10 11

OptiPrep™ Fraction

B

ng of LysMCCDM1 per 200,000 cells

0.15

0.10

0.05

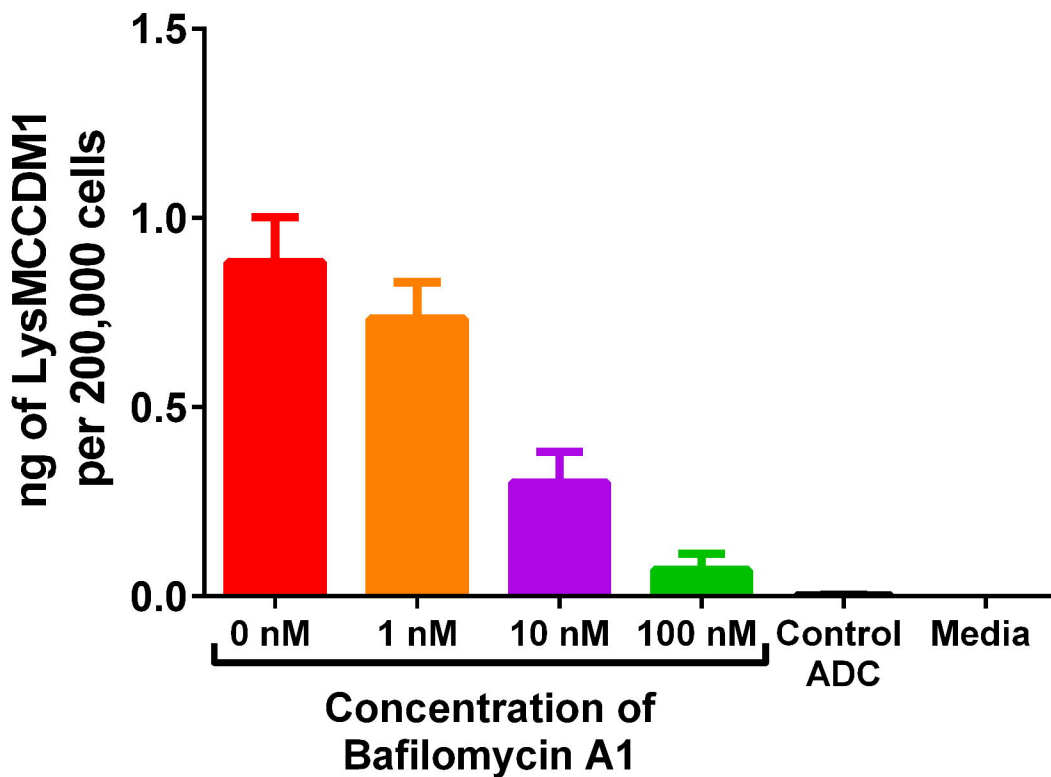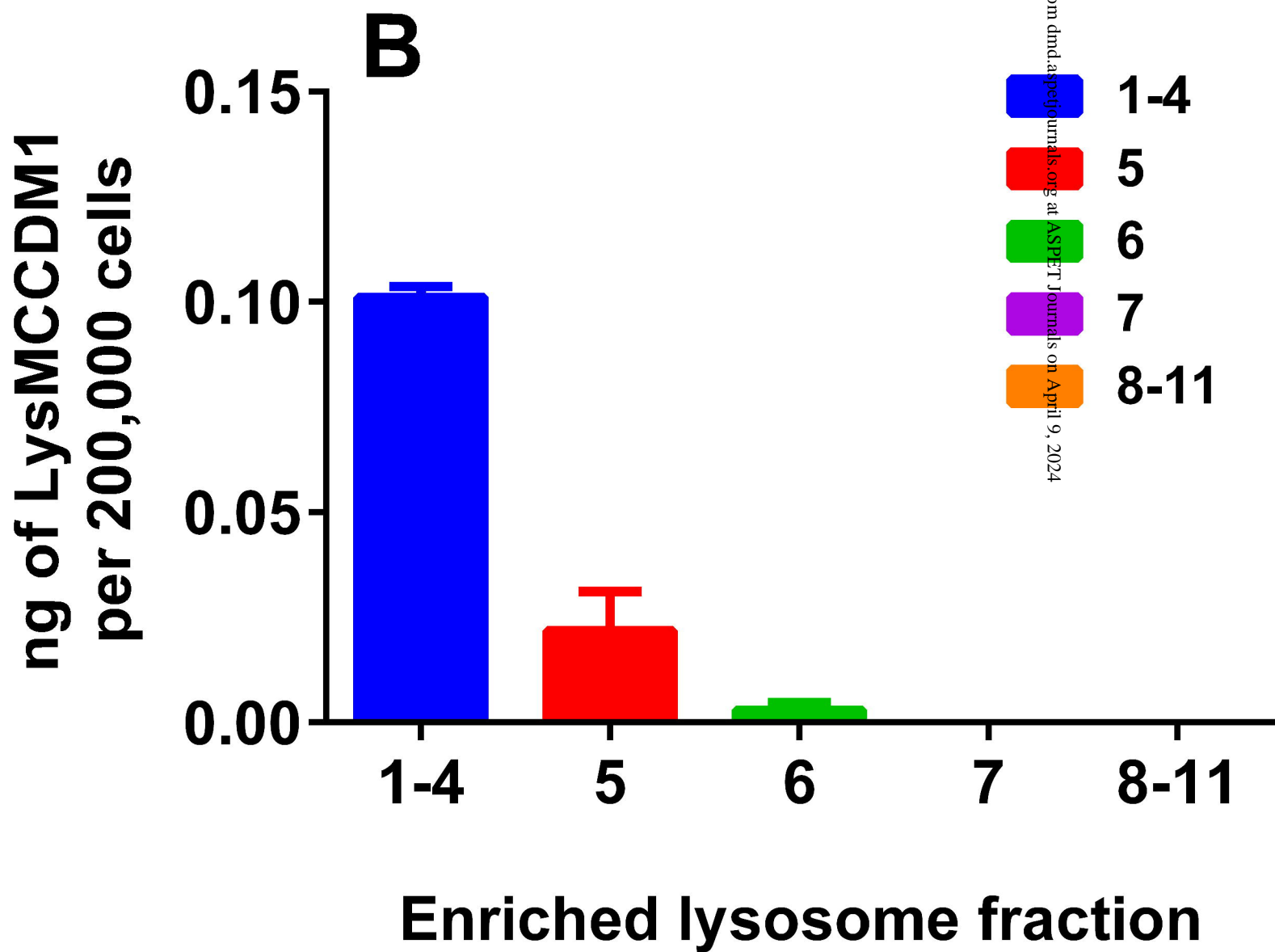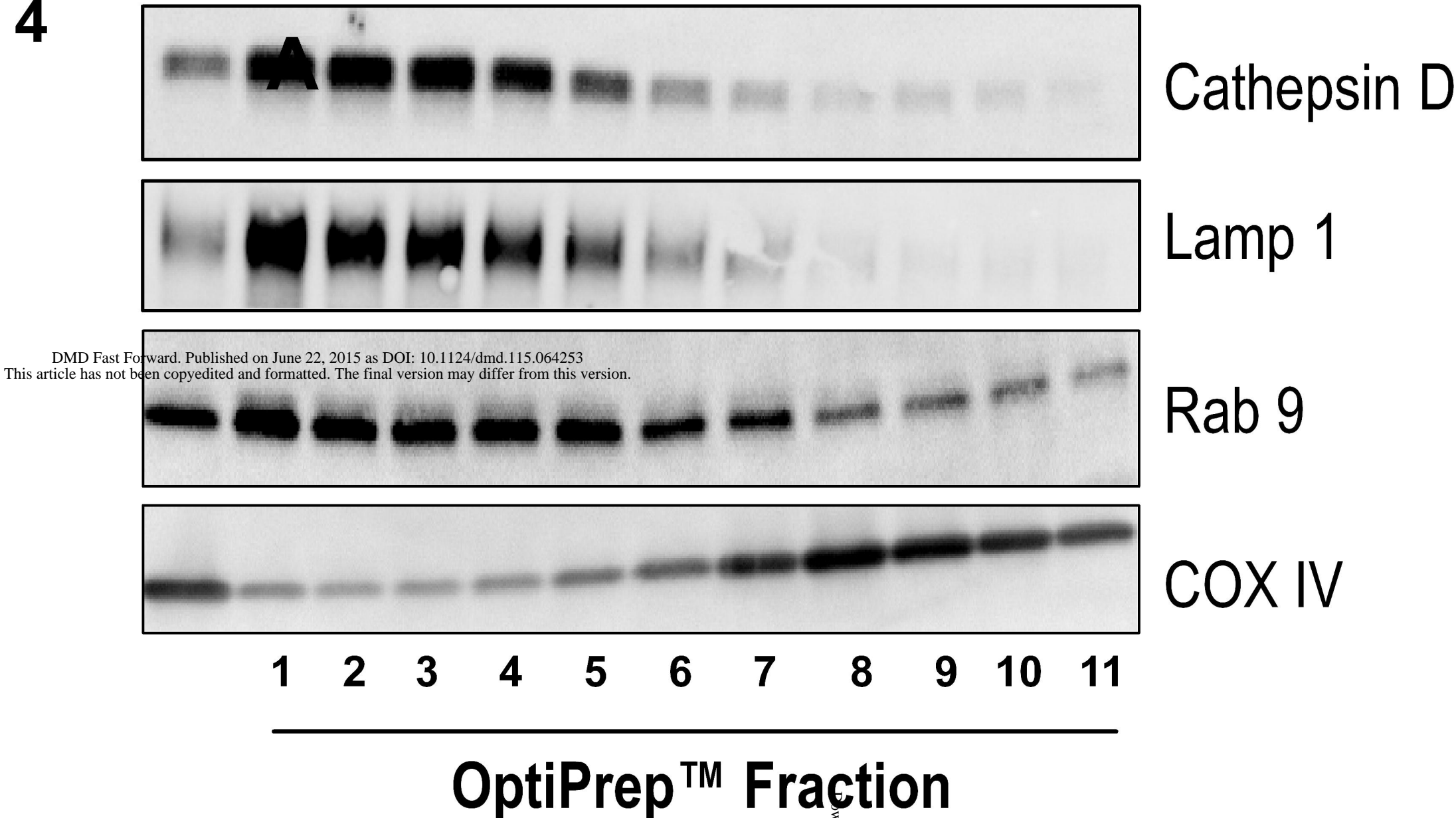0.00

1-4 5 6 7 8-11

1-4
5
6
7
8-11

Enriched lysosome fraction

DMD #64253

SUPPLEMENTAL DATA

SHORT COMMUNICATION: Drug Metabolism and Disposition

Intracellular Catabolism of an Antibody Drug Conjugate with a Non-Cleavable Linker

Brooke M Rock, Mark E Tometsko, Sonal K Patel, Kevin J Hamblett, William C Fanslow, Dan A Rock

Department of Pharmacokinetics and Drug Metabolism, Amgen, Inc, Seattle, WA

(BMR, DAR, SKP)

Therapeutic Innovation Unit, Amgen, Inc, Seattle, WA (KJH, MET, WCF)

Supplemental Figure 1.

10 nM [DM1] equivalence of anti-CD70 Ab-MCC-DM1 (ADC), media only, and ADC with varying concentrations of bafilomycin A (BAF) was added 786-0 cells. Following a 24 hr exposure cell viability was monitored continuously by Incucyte (Essen BioScience, Ann Arbor, MI). The percent confluence which correlates to cell viability is plotted in Supplemental Figure 1.
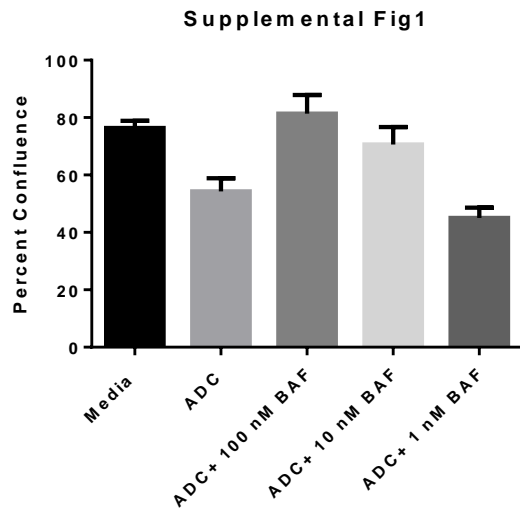
Supplemental Fig1

Supplemental Table 1

Measurement of Lys-MCC-DM1 after a 10 nM [DM1 eq] of anti-CD70 Ab-MCC-DM1 treatment to 786-0 cells for 24 hr, followed by enrichment of the lysosomal fraction. Percent Lys-MCC-DM1 was calculated by ng of Lys-MCC-DM1/ total ng of Lys-MCC-DM1 recovered.

Replicate	Percent of Lys-MCC-DM1			
	Cell Supernatant	Extraction from Cell Pellet	Enriched Lysosome	Total
1	2	7	80	89
2	4	6	84	94
3	1	12	80	93
4	3	11	79	93
Average	**2.5**	**7**	**82**	**91.5**
Standard Deviation	**1.3**	**2.9**	**2.2**	**2.2**

Supplemental Table 2

Apparently permeability ratios of Lys-MCC-DM1 (0.1, 1, 5, and 10 uM) in LLC-PK1 cells The parental cell line LLC-PK1(porcine renal epithelial cells) was purchased from American Type Culture Collection (ATCC, Manassass, VA). Potential transporter susceptibility for Lys-MCC-DM1 was measured in a vectorial apicalto-basolateral and basolateral-to-apical transport across parental LLC-PK1 transfected cells grown in monolayers on a porous membrane.

Concentration Lys-MCC-DM1 (uM)	A->B	SD	B->A	SD	Papp Avg (x10^{-6} cm/s)	ER	SD
0.1	3.7	0.2	4.7	0.4	4.2	1.3	0.1
1	1.6	0.1	1.9	0.1	1.7	1.2	0.1
5	1.1	0.1	1.2	0.2	1.2	1.1	0.1
1.0	1.0	0.1	1.1	0.2	1.0	1.1	0.2

*Mean of 3 studies
SD = standard deviation (n=3)
A>B = apical-to-basolateral transport
B>A = basolateral-to-apical transport